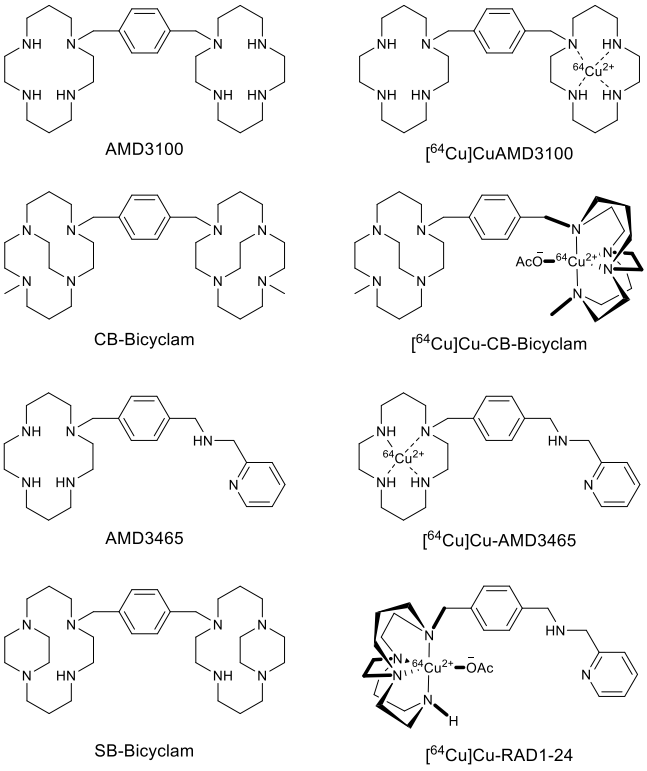

Supplemental Figure 1. Structures of bicyclam and related molecules including those of interest for imaging studies with copper-64 (right hand side)(*1-4*). The surface of CXCR4 is negatively charged, with aspartate and glutamate residues. Site direct mutagenesis has shown that AMD3100 (which is protonated at physiological pH) binds to two key residues on the external surface of CXCR4 (Asp171 and 262). The metal complexes are thought to switch the binding from hydrogen bonding to coordinate bond interactions. The transition metal complexes of AMD3100 generally have higher affinity for the receptor (zinc(II) and nickel(II)) although the advantage is reduced with copper(II) which is likely due to the longer weaker axial interaction(s) formed with the metal centre. Our theory (which has been validated in our previous studies on CB-Bicyclam and SB-Bicyclam and related compounds(*1,3,5-7*)) is that optimisation of the bonding and configurational fixing of the cyclam ring will provide higher affinity for the CXCR4 receptor. We have demonstrated that while SB-bicyclam and CB-bicyclam have low affinity for the CXCR4 receptor, on complex formation with cobalt(II), nickel(II), copper(II) and zinc(II) this is increased. The balance between affinity and clearance may be better met with the single metal centre derivative as, although the affinity is lower, the high stability will be retained and an electrostatic interaction is possible with the second protonated CB-cyclam ring. A further key advantage of forming the mono-copper compound by labelling the low affinity CB-bicyclam is that it can easily be separated from the precursor to give a high affinity tracer from a low affinity precursor. The investigation of the therapeutic characteristics of non-radioactive Cu_2CB-bicyclam is also underway showing in vivo that blocking of CXCR4 in murine models has a more profound effect than that AMD3100 alone, in line with the reported extended residence time at receptor.

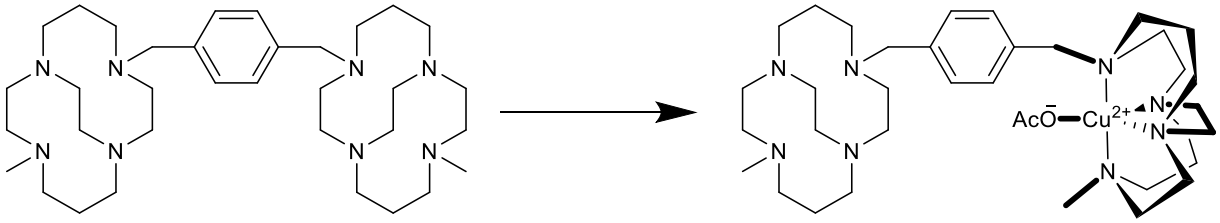

Supplemental Figure 2. Synthesis of CuCB-Bicyclam. 4-Methyl-11-[4-(4-methyl-1,4,8,11-tetraaza-bicyclo[6.6.2]hexadecylmethyl)-benzyl]-1,2,8,11-tetraaza-bicyclo[6.6.2]hexadecane tetrahydrochloride (CB-Bicyclam) was synthesised following literature protocols.(*1*) CB-Bicyclam (200 mg, 0.34 mmol) was dissolved in degassed dry methanol (30 mL), to this a dry methanolic solution (20 mL) of copper(II) acetate (60.8 mg, 0.33 mmol) was added dropwise. The solution was heated at reflux overnight after which the solvent was reduced *in vacuo* to ~5 mL and purified via size exclusion chromatography using Sephadex LH20 (GE Healthcare, UK) eluted with methanol, the coloured band fraction collected and dried *in vacuo* to yield a blue solid (90%, 212 mg) [The compound could also be purified by semi-prep as HPLC- see radiochemical synthesis for details]. HRMS: $[M - 2CH_3COO]^{2+}$ calcd. for $C_{34}H_{62}CuN_8$ m/z = 322.7191, found m/z = 322.7182. UV/vis. (CH_3CN) λ_{MAX} = 682 nm. Anal. calc. for $C_{36}H_{68}N_8CuO_4 \cdot 2HCl \cdot 2H_2O$: C 52.25; H 8.54; N 12.83. Measured C 52.14; H 8.40; N 12.77%. Analytical: 5%-95% MeOH (+0.1% TFA)/H2O (+0.1% TFA) in 20 min. 1 ml/min. RT = 11 min. (Column: ACE 5 C18 4.6 mm x 250 mm, 100Å, 5 µm).

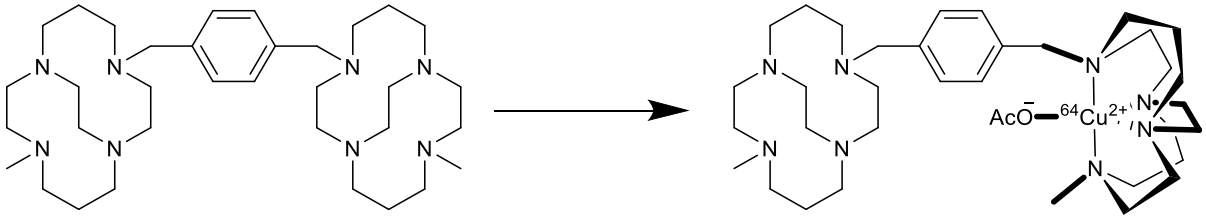

Supplemental Figure 3. Radiochemical synthesis of ^{64}Cu-CuCB-Bicyclam and stability. The ^{64}Cu-$CuCl_2$ solution was modified to ~pH 7 using NaOH and converted to ^{64}Cu-$Cu(OAc)_2$ by adding an equal volume of sodium acetate (0.4 M, pH 7) and heating at 60°C for 5 minutes. ~500 MBq was added to the reaction vial and an amount of CB-Bicyclam was added to ensure the reaction concentration of ligand was 0.5 mg/ml. The reaction was heated at 95°C and monitored by radio-TLC until full copper-64 incorporation was observed, between 30-45 minutes. ^{64}Cu-CuCB-Bicyclam was purified from excess CB-Bicyclam via semi-preparative HPLC using an Ace 5 C18, 250 x 10 mm, 100 Å, 5 μm column eluting with 25%-40% MeOH (+0.1% TFA)/H2O (+0.1% TFA) in 20 min at 4.7 ml/min (RT = 7.5 min), after which the solvent was removed, redissolved in PBS and sterile filtered. Lipophilicity assays were carried out using the shake-flask method using octanol and PBS. Acid stability was assessed by incubating ~5 MBq of synthesised tracer (^{64}Cu-CuAMD3100 or ^{64}Cu-CuCB-Bicyclam) in perchloric acid (6 M, 200 μl) at 37°C for 3 hours and measuring via radio-TLC using the same methods as in radiosynthesis.

Supplemental Table 1: List of primers used for SYBR Green qPCR.

Target	Sequences (5' – 3') or catalogues number	Supplier
hCXCR4	QT00223188	Qiagen
mCXCR4	QT00249305	Qiagen
18S	F: TAGAGGGACAA.GTGGCGTTC R: CGGACATCTAAGGGCATCAC	Sigma-Aldrich

Total RNA was extracted using an E.Z.N.A total RNA kit 1 (Omega Bio-tek) following the manufacturer's protocol, and then treated with RNase-free DNase I for genomic DNA contamination removal. RNA samples isolated were evaluated with a Nanodrop spectrophotometer for concentration, quantity and purity. About 1 µg high-quality total RNA was reverse-transcribed into single-strand cDNA in a 20 µL reaction mix with QuantiTect Reverse Transcription kit (QIAGEN). RT-qPCR amplification was carried as follows: 20 ng cDNA was mixed with 10 µL 2x QuantiTect SYBR Green PCR Master Mix, 1 µL QuantiTect Primer (table 1) and water to give a total volume of 20 µL. The reaction condition was as follows: 95°C for 15 minutes, 94°C for 15 seconds, 55°C for 30 seconds, 72°C for 30 seconds, with a total 40 cycles.

(a)

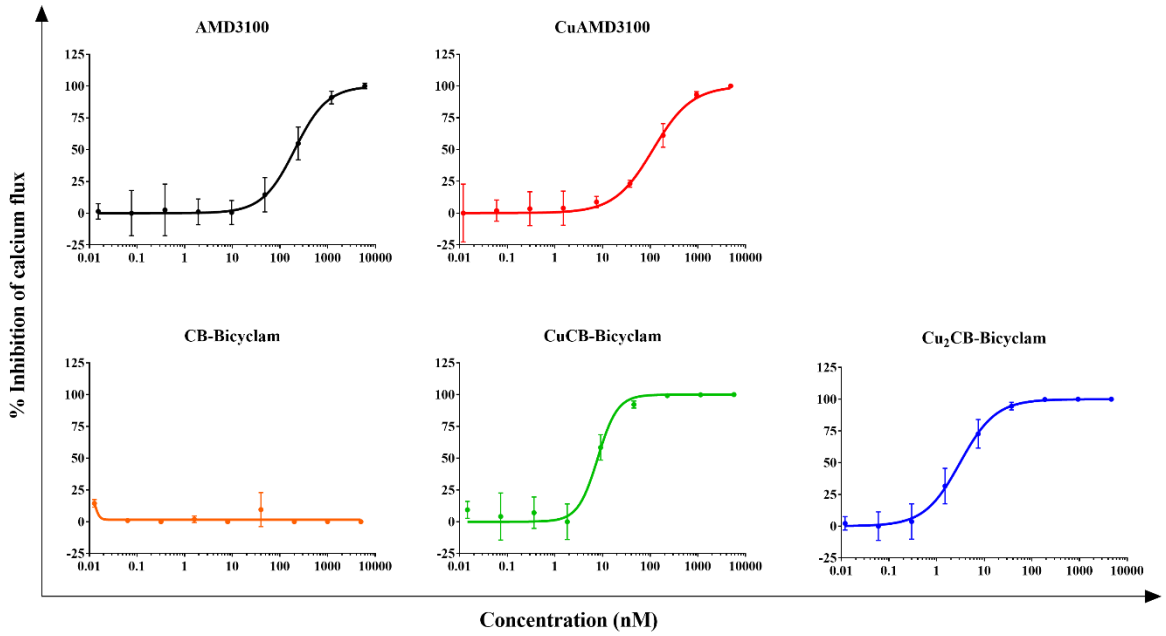

(b)

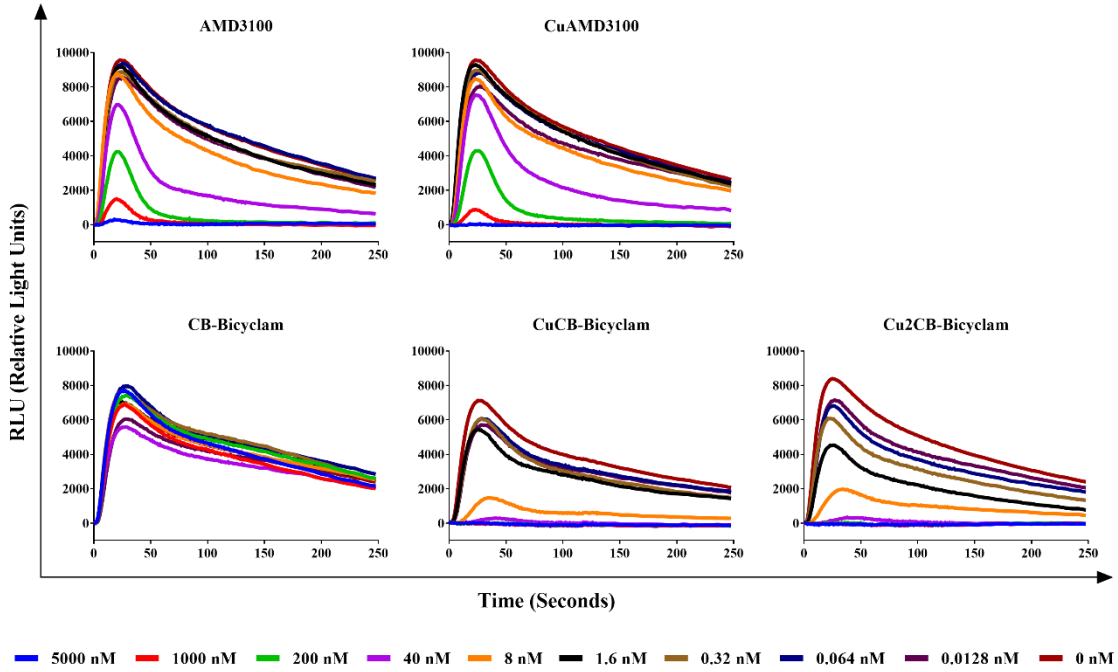

Supplemental Figure 4. (a) Calcium flux experiment dose-response curves for human CXCR4 signalling in response to CXCL12 stimulation after addition of the potential antagonist compounds. The dose response curves presented are the combined results of five biological repeats (each on different assay plates on different days) for each compound with three internal replicates in a single plate. (b) Fluorescence vs time plots for the calcium flux assay. An example calcium flux time plot is given for each compound with the nine concentrations plotted on each along with a control where no compound is added.

(a)

Compound	Murine CXCR4 binding IC_{50} (nM)
AMD3100	9.263 ± 0.730
CuAMD3100	17.01 ± 0.88
CB-Bicyclam	> 5000
CuCB-Bicyclam	1.791 ± 0.112
Cu_2CB-Bicyclam	0.5973 ± 0.0990
Pentixafor	> 5000

(b)

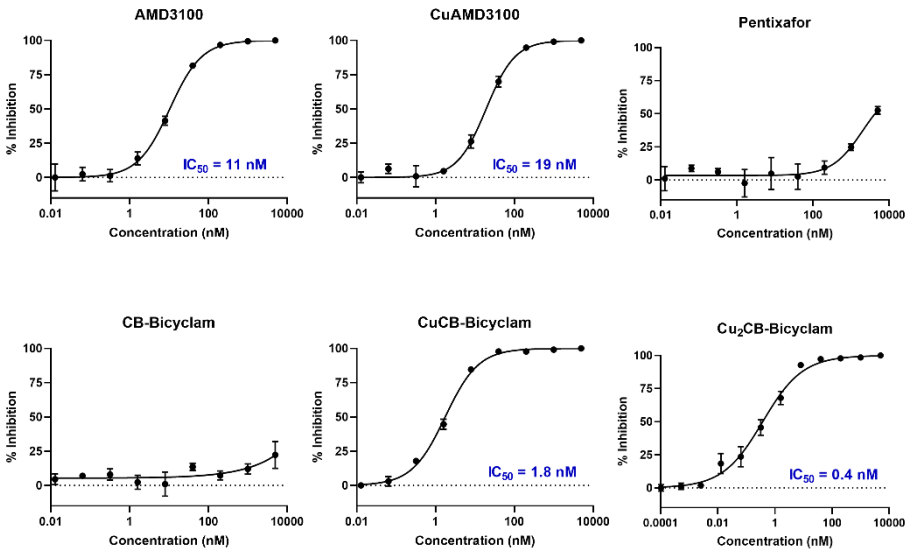

Supplemental Figure 5. (a) Chemokine (mouse $CXCL12^{AF647}$) binding inhibition assay IC_{50} results in murine CXCR4 cell line. (b) Example dose response curve from one of the experimental data sets for the chemokine binding inhibition assays. U87-MG cells stably transfected with mouse CXCR4 were washed once with assay buffer (Hanks' balanced salt solution with 20 mM HEPES buffer and 0.2% bovine serum albumin, pH 7.4) and then incubated for 15 min at room temperature with the sample diluted in assay buffer at the indicated concentrations. Subsequently, mouse $CXCL12^{AF647}$ ($mCXCL12^{AF647}$) was added to the compound-incubated cells at 50 ng/ml. The cells were incubated for 30 min at room temperature. Thereafter, the cells were washed twice in assay buffer, fixed in 1% paraformaldehyde in PBS, and analyzed on FACSCanto flow cytometer (Becton Dickinson, San Jose, CA, USA). The percentages of inhibition of $mCXCL12^{AF647}$ binding were calculated according to the formula: $[1 – ((MFI – MFI_{NC}) / (MFI_{PC} – MFI_{NC}))] \times 100$ where MFI is the mean fluorescence intensity of the cells incubated with $mCXCL12^{AF647}$ in the presence of the inhibitor, MFI_{NC} is the mean fluorescence intensity measured in the negative control (i.e., autofluorescence of unlabeled cells), and MFI_{PC} is the mean fluorescence intensity of the positive control (i.e., cells exposed to $mCXCL12^{AF647}$ alone).

(a)

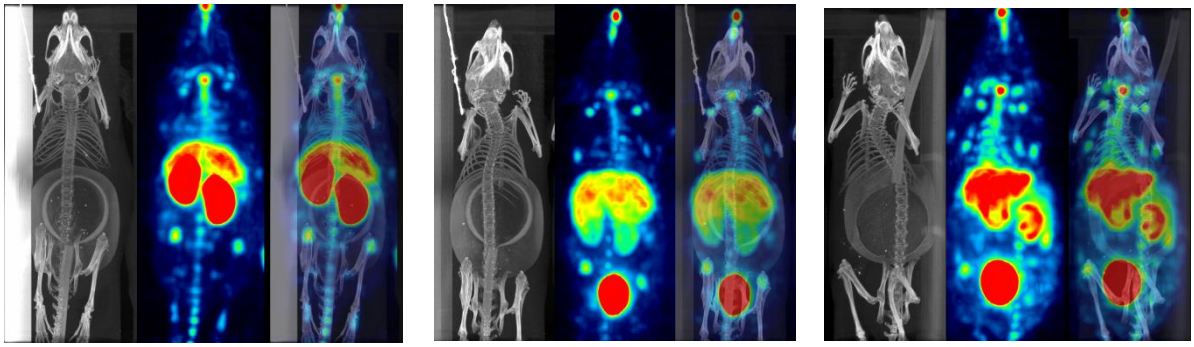

(b)

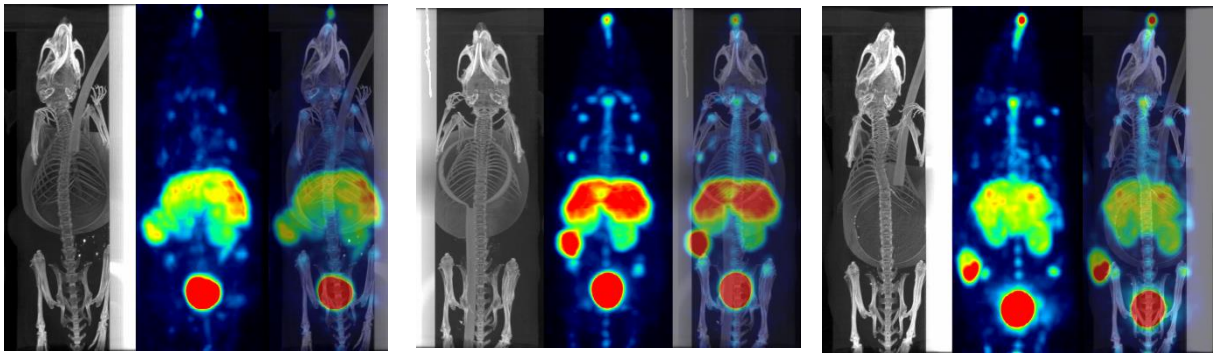

(c)

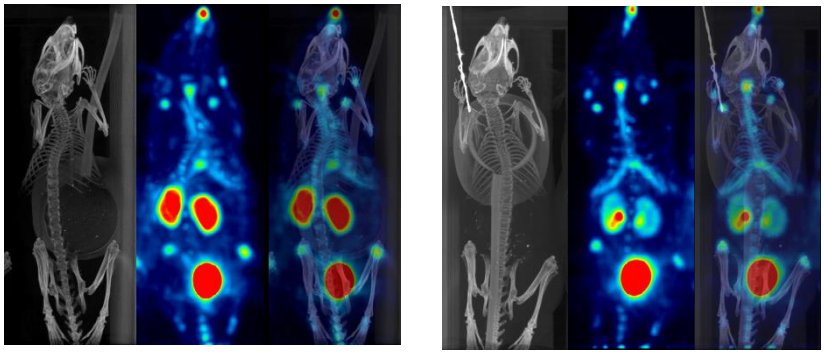

Supplemental Figure 6. In vivo PET/CT evaluation of ^{64}Cu-CuCB-Bicyclam in all animals. (A) Fused PET-CT maximum intensity projections at 70-90 mins post-injection from CD1 mice bearing (a) U87 (n=3) (b) U87-CXCR4 (n=3), and (c) U87.CXCR4 block (n=2) (SUV 6.5). Animals were injected with 9.6 ± 0.7 MBq of ^{64}Cu-CuCB-Bicyclam. Blocking dose of 5 mg/Kg of Cu_2CB-Bicyclam given 1 hour prior to ^{64}Cu-CuCB-Bicyclam injection where indicated.

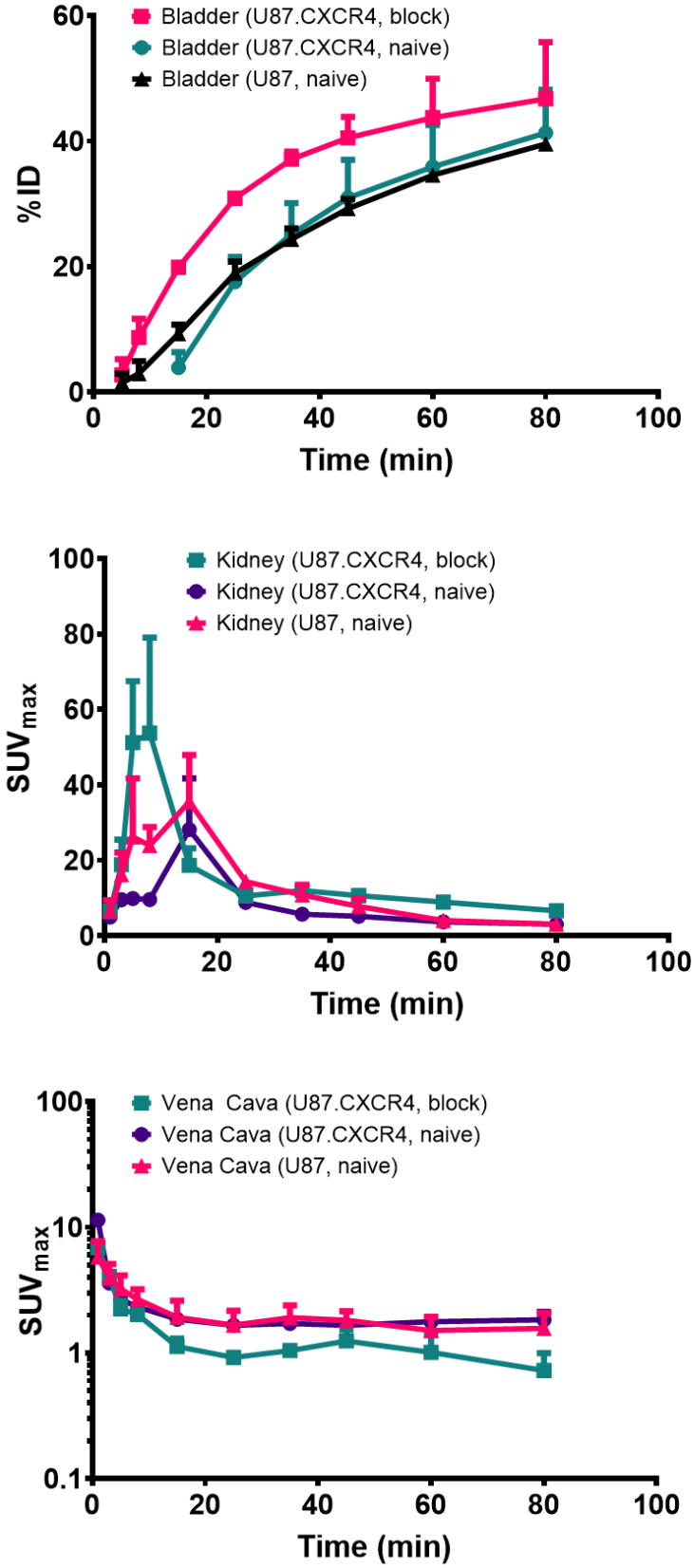

Supplemental Figure 7. Dynamic time activity curves showing uptake of ^{64}Cu-CuCB-Bicyclam in bladder (top), kidney (middle) and vena cava (bottom) during 80 minutes. Data represent mean uptake of n=2-3 animals ± SEM.

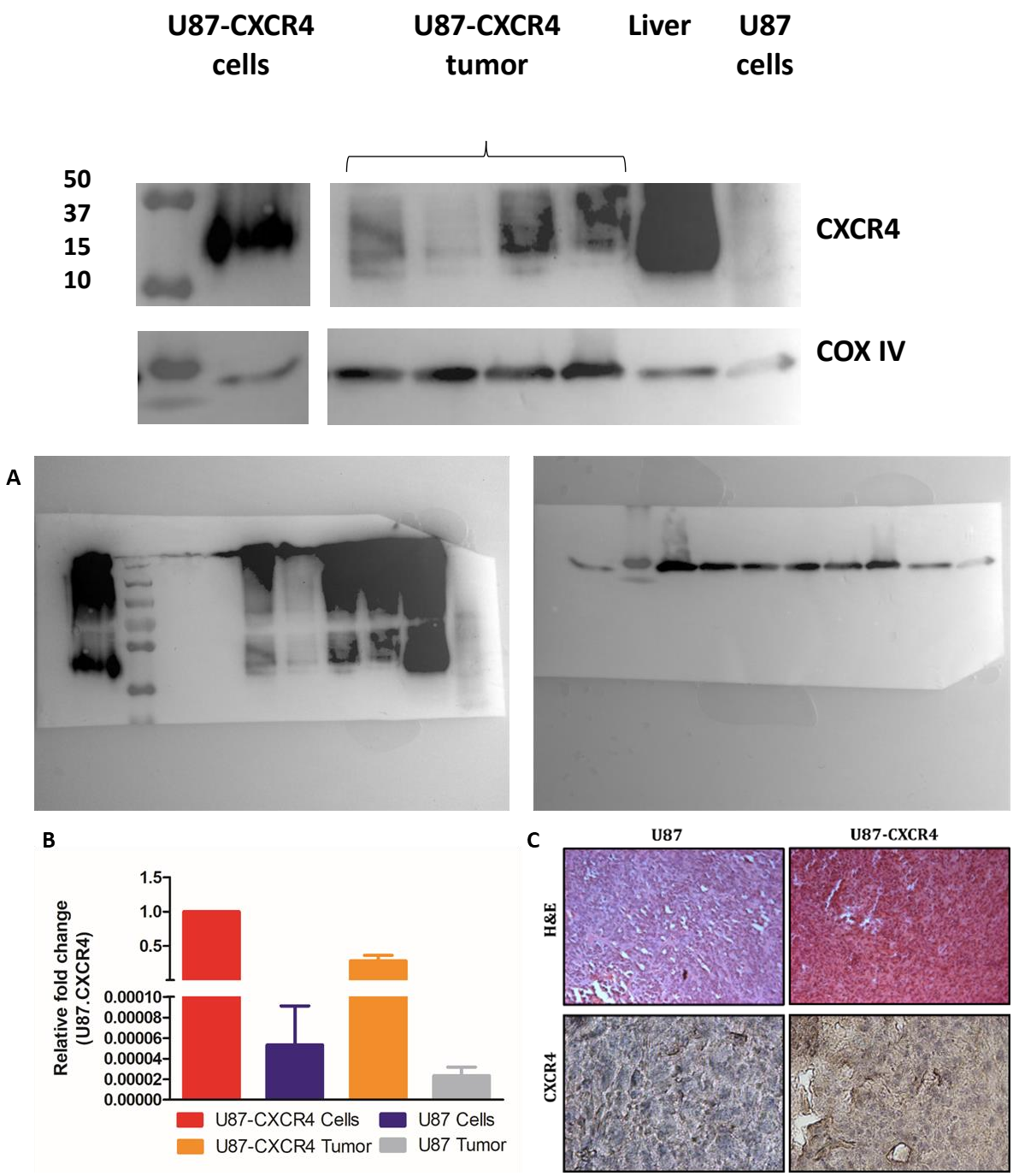

Supplemental Figure 8. Ex vivo analysis of tumor by (A) western blot (original gels for CXCR4 (left) and COX IV loading control (right) Lanes: *1* U87-CXCR4 cell lysates; *2* MW markers; *3-8* U87.CXCR4 tumor lysates; *9* Liver lysate; *10* U87 cells), (B) qPCR and (C) immunohistochemistry.

Supplemental Table 2: Ex-vivo biodistribution of ^{64}Cu-CuCB-Bicyclam after blocking with a range of agents. Data are mean of two animals ± SD.

Table 1

Biodistribution of [^{64}Cu]CuCB-Bicyclam after blocking

Block time		60 min				12 hours			
Block agent	**Naïve**	**Cu_2-CB**	**Cu-CB**	**AMD3100**	**AMD3465**	**Cu_2-CB**	**Cu-CB**	**AMD3100**	**AMD3465**
Organ/tissue									
Blood	0.59 ± 0.00	0.32 ± 0.10	0.39 ± 0.06	0.36 ± 0.08	0.31 ± 0.31	0.36 ± 0.17	0.37 ± 0.01	0.62 ± 0.57	0.48 ± 0.11
Brain	0.07 ± 0.00	0.04 ± 0.01	0.06 ± 0.00	0.07 ± 0.00	0.13 ± 0.07	0.05 ± 0.02	0.06 ± 0.00	0.07 ± 0.02	0.07 ± 0.01
Heart	0.67 ± 0.10	0.39 ± 0.11	0.53 ± 0.06	0.51 ± 0.09	0.70 ± 0.28	0.42 ± 0.08	0.51 ± 0.01	0.51 ± 0.05	0.71 ± 0.13
Muscle	0.18 ± 0.01	0.10 ± 0.01	0.47 ± 0.19	0.13 ± 0.01	0.21 ± 0.06	0.46 ± 0.41	0.29 ± 0.20	0.45 ± 0.47	0.17 ± 0.08
Lungs	2.89 ± 0.03	1.06 ± 0.53	1.71 ± 0.47	1.91 ± 0.06	2.91 ± 1.06	1.23 ± 1.50	2.35 ± 0.18	2.55 ± 0.74	2.93 ± 0.72
Thymus	1.73 ± 0.04	0.33 ± 0.11	0.45 ± 0.10	0.72 ± 0.03	1.36 ± 0.23	1.05 ± 0.35	1.14 ± 0.16	0.64 ± 0.01	1.03 ± 0.58
Bone	1.42 ± 0.04	0.63 ± 0.08	0.80 ± 0.42	0.89 ± 0.18	1.26 ± 0.37	0.98 ± 0.15	0.91 ± 0.06	1.24 ± 0.21	1.93 ± 0.06
Spleen	4.71 ± 0.30	0.48 ± 0.11	0.78 ± 0.00	2.52 ± 0.49	3.81 ± 1.17	2.52 ± 0.21	3.12 ± 0.16	3.53 ± 0.91	3.67 ± 0.98
Nose	1.26 ± 0.14	0.94 ± 0.41	2.41 ± 0.66	0.89 ± 0.21	1.32 ± 0.66	0.84 ± 0.16	1.19 ± 0.22	1.09 ± 0.25	1.17 ± 0.81
Kidney	8.11 ± 2.06	6.52 ± 1.36	7.11 ± 1.09	5.51 ± 1.70	4.89 ± 0.73	5.04 ± 1.26	3.40 ± 0.33	5.33 ± 0.69	4.54 ± 2.83
Liver	13.77 ± 4.20	3.40 ± 1.89	4.61 ± 1.50	13.59 ± 5.71	18.56 ± 5.18	14.98 ± 4.88	17.60 ± 1.34	17.91 ± 1.16	19.14 ± 2.92
Intestines	3.68 ± 0.10	1.59 ± 0.61	1.79 ± 0.12	1.91 ± 0.23	1.90 ± 0.26	1.36 ± 1.12	1.39 ± 0.44	1.68 ± 0.06	1.86 ± 0.25

References

1. Khan A, Nicholson G, Greenman J, et al. Binding optimization through coordination chemistry: CXCR4 chemokine receptor antagonists from ultrarigid metal complexes. *J Am Chem Soc.* 2009;131:3416-3417.

2. Nimmagadda S, Pullambhatla M, Stone K, Green G, Bhujwalla ZM, Pomper MG. Molecular imaging of CXCR4 receptor expression in human cancer xenografts with [64Cu]AMD3100 positron emission tomography. *Cancer Res.* 2010;70:3935-3944.

3. Valks GC, McRobbie G, Lewis EA, et al. Configurationally restricted bismacrocyclic CXCR4 receptor antagonists. *J Med Chem.* 2006;49:6162-6165.

4. Woodard LE, De Silva RA, Azad BB, et al. Bridged cyclams as imaging agents for chemokine receptor 4 (CXCR4). *Nucl Med Biol.* 2014;41:552-561.

5. McRobbie G, Valks GC, Empson CJ, et al. Probing key coordination interactions: configurationally restricted metal activated CXCR4 antagonists. *Dalton Trans.* 2007:5008-5018.

6. Smith R, Huskens D, Daelemans D, et al. CXCR4 chemokine receptor antagonists: nickel(II) complexes of configurationally restricted macrocycles. *Dalton Trans.* 2012;41:11369-11377.

7. Maples RD, Cain AN, Burke BP, et al. Aspartate-based CXCR4 chemokine receptor binding of cross-bridged tetraazamacrocyclic copper(II) and zinc(II) complexes. *Chem Eur J.* 2016;22:12916-12930.